

# Research and Development of a Special Slag Glass Ceramics

Baowei Li<sup>1</sup>, Ming Zhao<sup>1,\*</sup>, Yongsheng Du<sup>2</sup>, Hua Chen<sup>2</sup>, Jing Gao<sup>1</sup>, Hongxia Li<sup>1</sup>, Xiaolin Jia<sup>3</sup>

<sup>1</sup>Key Laboratory of Integrated Exploitation of Bayan Obo Multi-Metal Resources, Inner Mongolia University of Science & Technology, Baotou, People's Republic of China

<sup>2</sup>College of Science, Inner Mongolia University of Science & Technology, Baotou, People's Republic of China

<sup>3</sup>School of Materials Science, Zheng Zhou University, Zhengzhou, People's Republic of China

## Email address:

lbaowei@126.com (Baowei Li), philip@imust.edu.cn (Ming Zhao), 46588582@qq.com (Yongsheng Du), kidsea@163.com (Hua Chen), gaojin@163.com (Jing Gao), hongxialea@163.com (Hongxia Li), jiaxxxlin@163.com (Xiaolin Jia)

\*Corresponding author

## To cite this article:

Baowei Li, Ming Zhao, Yongsheng Du, Hua Chen, Jing Gao, Hongxia Li, Xiaolin Jia. Research and Development of a Special Slag Glass Ceramics. *Engineering and Applied Sciences*. Vol. 3, No. 3, 2018, pp. 53-63. doi: 10.11648/j.eas.20180303.11

Received: June 6, 2018; Accepted: June 25, 2018; Published: July 25, 2018

---

**Abstract:** This paper is a thorough summary of the main results of the research group of the current authors, i.e. Research Group of Mining & Metallurgy Wastes Green-utilization with High-added Value, on developing glass ceramics of pyroxene system using Bayan Obo mine tailing and the fly ash from a Baotou thermal power plant as the main starting materials. The fabricating procedure and the typical properties were reported firstly. Then the primary effects of iron, lanthanum, cerium, niobium oxides and microwave sintering were examined respectively. Several important phenomena discovered during the research were analyzed. Based on these discoveries, the reason to the general good properties this special glass ceramic characterized by high hardness and bending strength, strong resistances to erosion and corrosion of acid and alkaline solutions was revealed. The result of the current study can serve as an example for the future utilization of solid wastes from mining, metallurgy and other relevant industries in a more profitable way and for the protection of both environment and natural resources.

**Keywords:** Glass Ceramics, Research and Development, Bayan Obo Mine Tailing

---

## 1. Introduction

Bayan Obo mine is a world-renowned multi-metal ore containing more than 70 elements in form of over 100 different minerals. Among them, iron, several Rare Earth (RE) elements, niobium, thorium, potassium, sodium and fluorine are of great industrial utilization value. The existence of these elements within Bayan Obo mine has characteristics of “low” in their concentration, “fine” in the average size of their relevant mineral and “complicated” in distribution [1]. The utilization of Bayan Obo resources started from iron in 1960s. Later in 1990s, RE became another exploitation target. With this process, a great amount of solid wastes, such as tailing, blast furnace slag and fly ash, has been produced and accumulated without a proper treatment, posing as a serious threat to both people and environment surrounding the

reserving area for those wastes [2].

How to effectively utilize these wastes may have dramatic influence in the development of local economy and society. Aiming to solve this problem, the research group of the current authors started relevant research work on the turn of the new millennium. It is well known, the relative open structure of oxide based material has made it is possible for the absorption of alien ions into their structure through ion substitution or directly entering the interstitial. By harnessing this special microstructural feature of oxide based materials, a special glass ceramic has been successfully prepared from Bayan Obo tailing and fly ash through the traditional glass melting progress with additional nucleation and crystallization heat-treatments [3-9]. The resultant material shows a good tolerance to the compositional complexity of the raw materials, and these two solid wastes can account for more than 50 wt%

of the total raw materials. The element assemblages in this material are far more complicated than just more than five of high entropy metal glasses. Therefore, the concept of high entropy can be well extended to such glass ceramics developed from solid wastes, though the mole ration of each element in such glass ceramic doesn't equal to those of others as in high entropy metal glass. More importantly, this special glass ceramic has a general superiority in its hardness, bending strength, and the resistance to abrasion, acid or alkaline erosion. Based on these successes, more than 20 innovation patents have been issued. Moreover, a pilot plant has been established for the production of glass ceramic plate, pipe, and straight glass ceramic lined steel pipe, and those in shape of three-way, union tee reducer and elbow. These products have been successfully applied in industries of metallurgy, construction, cement and chemical engineering. The life span of these products is at least five times of those of originally used nylon, tantalum or anti-abrasion steels. As a result, considerable revenue has been created for users of those products. The standard named "Slag Glass Ceramic Pipe" has authorized as the national standard for the construction industry of China (JC/T 2283-2014).

The aim of this paper is to provide a thorough summary on the important discoveries made by the research group of the current authors in the process achieving above-mentioned successes. It can further improve the research and

development of novel glass ceramic materials in addition to serves as a valuable reference for solid waste re-utilization and environment protection.

## 2. Experimental Procedure

### 2.1. Sample Preparation

The compositions of Bayan Obo tailing and the fly ash collected in a local thermal power plant are presented in Table 1. Based on it, a glass of the iron bearing pyroxene system was selected as the base glass. Its composition was shown in Table 2. This base glass was named as GS0. The raw materials used to fabricate this base glass were listed as following (all in weight percentage: wt%): 46.68 Bayan Obo tailing, 11.67 fly ash, 24.85 industrial-grade silica sand, 9.00 CaO, 4.25 Borax, CaF<sub>2</sub>, and 0.4 Cr<sub>2</sub>O<sub>3</sub>. In order to investigate the effect of La, Ce, three typical valuable elements of Bayan Obo tailing, another two batches of samples were prepared. The batch with additionally doped La<sub>2</sub>O<sub>3</sub>/CeO<sub>2</sub> (0.7 wt%, mole ratio of La<sub>2</sub>O<sub>3</sub>/CeO<sub>2</sub> =1:2) was named as GS1. In the case of Nb-related study and that of investigating the effect of microwave heating, a slightly modified GS0 formula (a base glass of diopside system) were used, and the corresponding batch was name GS0', and the batch with further addition of 0.5 wt% Nb<sub>2</sub>O<sub>5</sub> was named as GS2.

**Table 1.** Constituents of Bayan Obo tailing and the fly ash used in this study.

Constituents	MgO	Al <sub>2</sub> O <sub>3</sub>	SiO <sub>2</sub>	CaO	Fe <sub>2</sub> O <sub>3</sub>	R <sub>2</sub> O	P <sub>2</sub> O <sub>5</sub>	Loss	Other
Tailings	11.76	1.89	14.21	15.87	16.56	2.71	1.65	25.59	9.76
Fly ash	0.78	30.71	51.68	3.90	8.60	2.28	-	-	-

**Table 2.** Composition of the base glass in this study.

SiO <sub>2</sub>	CaO	Al <sub>2</sub> O <sub>3</sub>	MgO	Fe <sub>2</sub> O <sub>3</sub>	CaF <sub>2</sub>	Na <sub>2</sub> O	K <sub>2</sub> O
50.00	20.00	5.57	7.31	6.47	6.00	1.65	1.00

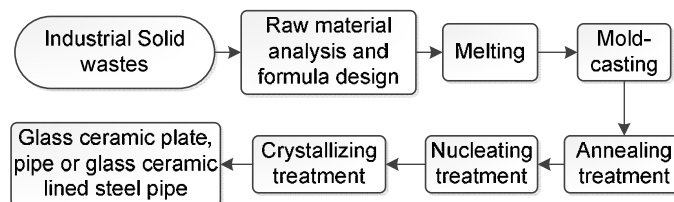


**Figure 1.** Flow chart of the procedure for manufacturing glass ceramic plate, pipe or glass ceramic lined steel pipe.

A modified glass melting-casting procedure was used to prepare the glass ceramics for this study. Figure 1 depicts the flow chart of this procedure. It can be further adapted with ease for manufacturing products with complicated shape at a pilot plant or an industrial production line.

As shown in Table 2, the as designed base glass of the iron-bearing pyroxene system falls under the category of the typical high silica system. However, it also contains a considerable amount of CaO, K<sub>2</sub>O, and Na<sub>2</sub>O. These oxides are most commonly used flux in glass industry. Therefore, after melting the raw material at 1450°C for three hours, a bubble-free glass melt can be obtained. Then the melt was into a mold of as designed shape and transferred with the mold

immediately into a furnace pre-heated at 600°C, in which the resultant glass was annealed for another three hours to release the inner stress generated during the casting process. Frit of the water quenched base glass melt was analyzed by a differential scanning calorimeter (DSC- NETZSCH STA 449C). The result shown in Figure 2 indicates glass transition ( $T_g$ ) emerged at 635°C, and the temperature at which the primary crystalline phase crystallizing at its peaking rate ( $T_p$ ) was at 825°C. Based on these two results and the common practice of peer researchers, 670 and 825°C were selected for the nucleating and crystallizing heat-treatment respectively, and the soaking times were unanimously set as two hours. After the heat-treatment, the power to the furnace was turned

off, allowing the obtain pyroxene glass ceramics to be cooled to the room temperature within the furnace naturally.

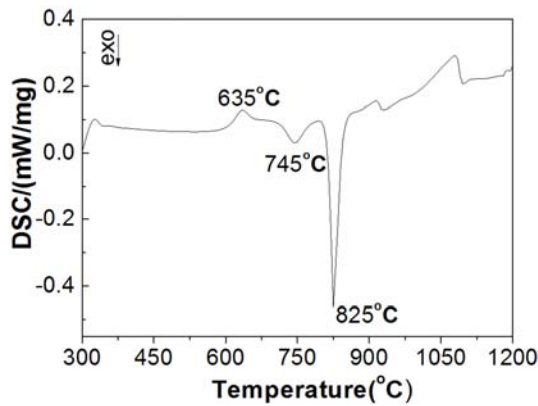


Figure 2. DSC curve of the water quenched base glass.

## 2.2. Microstructure and Property Characterizations

The assemblage of the crystalline phase of the glass ceramics was determined on a Panalytical X'pert powder X ray diffraction spectrometer. The surface morphology was observed on a Zeiss Supra 55 FESEM. Prior to such examination, the etched (5% HF solution for 20s) cross-section of the heat-treated sample was made electrically conductive by gold-coating. Tecnai G2 F20 STwin scanning transmission electron microscope (STEM) and its EDS attachment were also used to gather the microstructural and compositional information. The bending strength was

measured on a CSS-88000 universal mechanical property tester. The density, hardness and resistance to abrasion, and the stability against acid or alkaline erosion were tested according to the corresponding national standards of China.

## 3. Results

### 3.1. Brief History of the Relevant Research

Figure 3 depicts the brief history of the search group of the current authors on developing special glass ceramics from different industrial solid wastes. It has been through three stages. The research within the first stage, starting from 2000 to 2007, was of the theoretical category. In the next stage (2008-2012), some major advances were achieved in technology exploration and integration for larger-scale fabrication of slag glass ceramics and the establishment of a pilot plant. The third stage from 2013 until now witnessed the breakthroughs of the current authors in the theoretical study and in-situ application of some of pilot plant products in industries of metallurgy, cement and chemistry. Typical properties of the special glass ceramic fabricated from Bayan Obo tailing and the aforementioned fly ash were summarized in Table 3.

It shows this special material has a characteristic of high hardness and bending strength, outstanding resistance to abrasion and strong stability against acid and alkaline erosion. The general property of this special material is already superior to those of other glass ceramics, natural marble or granite [10-18].

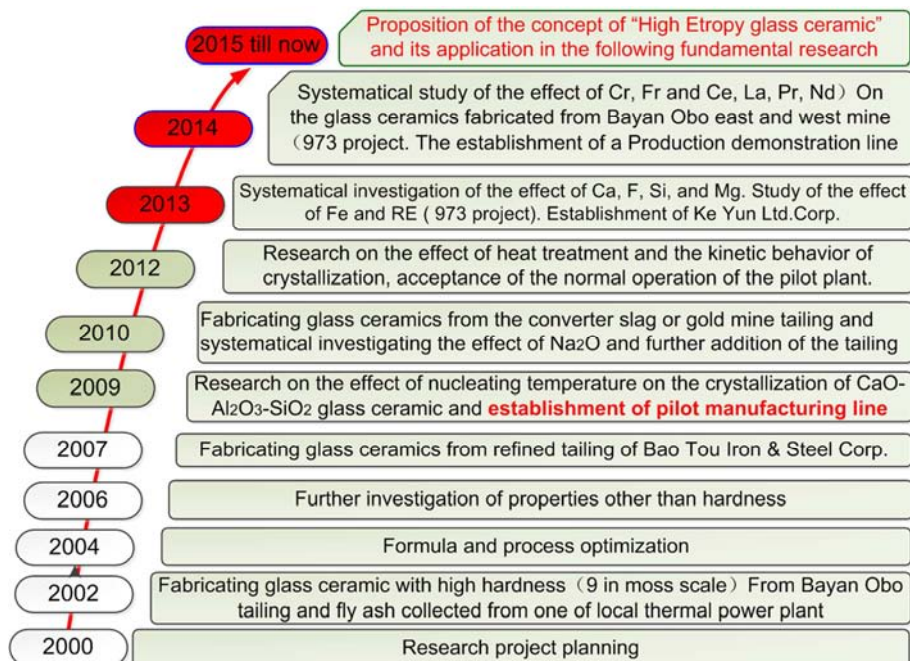
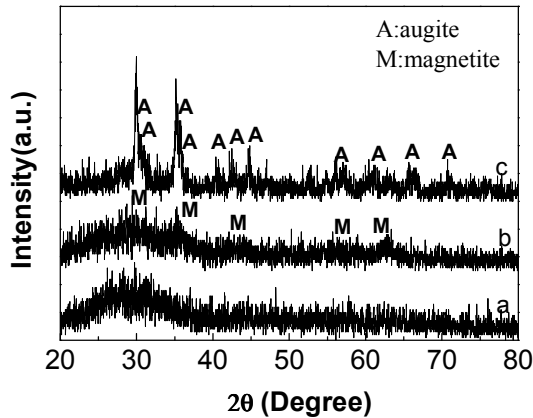


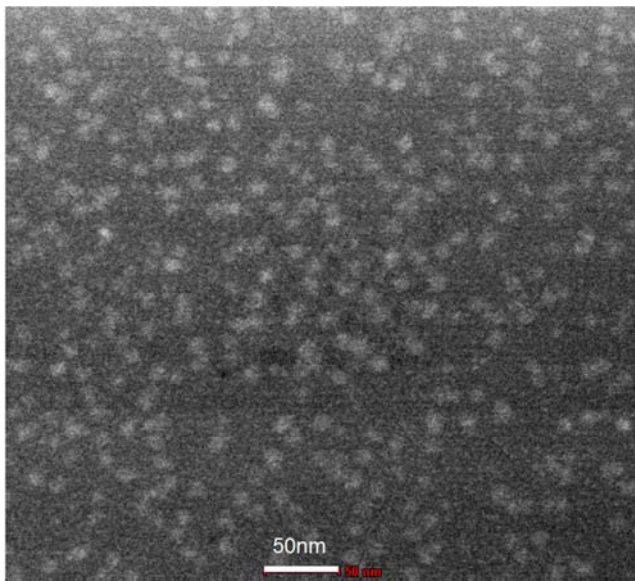
Figure 3. Brief history of the search group of the current authors on developing special glass ceramics from different industrial solid wastes.

Table 3. Properties of the slag glass ceramic products manufactured in the pilot plant established by the research group of the current authors.

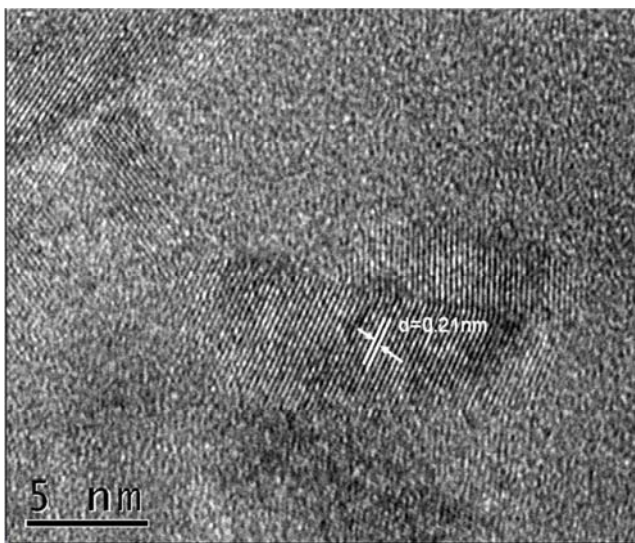
Tested item	Moss hardness	Bending strength (MPa)	Density (g/cm <sup>3</sup> )	Abrasion (g/cm <sup>3</sup> )	Acid Resistance (H <sub>2</sub> SO <sub>4</sub> , 1.84g/cm <sup>3</sup> )	Alkaline resistance (NaOH, 20%)
Result	9	198	3.21	0.04	99.9%	97.7%
Referenced standard	JC/T872-2000	JT/T263-93	GB/T 3810.3-2006	JC/T260-2001	JC/T258-93	JC/T258-93



**Figure 4.** XRD pattern of the base glass of the GS0 group, a) water quenched after melting, b) nucleated, c) crystallized.



(a) STEM



(b) HRTEM

**Figure 5.** STEM and HRTEM photos of the nucleated sample of GS0 group.

### 3.2. The Mechanism of $Fe_2O_3$ Enhancing the Nucleation

Bayan Obo tailing still contains a considerable amount of iron. It will normally be oxidized to  $Fe_2O_3$  in the high-temperature process of glass ceramics fabrication. Peer studies have shown  $Fe_2O_3$  is a key factor to the nucleation and crystallization of the pyroxene based glasses [19-25]. However, detailed mechanism is yet to be revealed.

Therefore, the crystalline phase assemblages of three GS0 samples, which have been separately annealed, nucleated or crystallized, were examined to reveal the effect of  $Fe_2O_3$ . The result was present in Figure 4. The curve a) in this figure shows the XRD pattern of the sample GS0 only consists of diffuse reflectance spectra, indicating no detectable crystalline has formed after the annealing procedure. Contrarily, several weak diffraction peaks of magnet (Marked by M) emerge on pattern b, while several distinctive diffraction peaks of augite arise from the pattern c. These results in combination indicate the microstructure evolution should be in the order of glass to magnet, and then to augite. In order to further verify this theory, one nucleated GS0 sample was examined by the aforementioned HRTEM operating in the STEM mode. The results were shown in Figure 5.

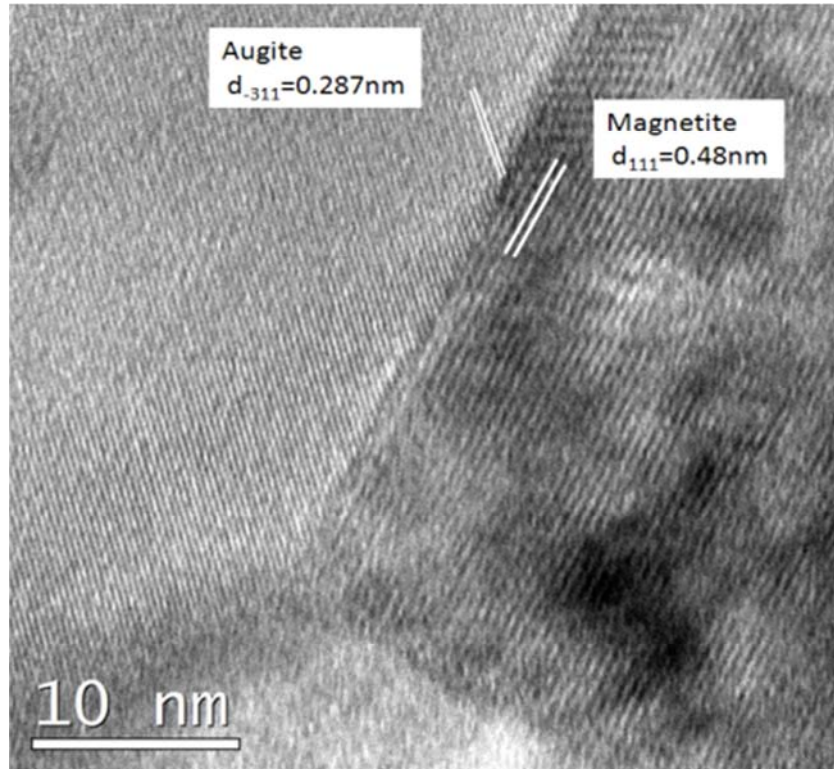
The TEM photo marked by 5 (a) shows there are a great deal of white spherical particles embedding in the gray matrix. The further magnified STEM picture (5(b)) reveals those white spheres of around 10nm are actually the region with long range periodicity, in which the inter-planar distance equals to 0.21nm. This distance is in accordance of the inter-planar spacing of (400) crystal planes of a magnet crystal. This result, together with above XRD analysis, indicates those white spheres are of a nano magnet crystal in nature.

One of typical HRSTEM photos of a crystallized sample of GS0 group was shown in Figure 6. It reveals a grain boundary formed by two different grains closely adhere to each other. On the left, is a grain with the inter-planar spacing of 0.287nm, while the grain on the right shows an inter-planar spacing of 0.48nm. These two values equal to the inter-spacing of the ( $\bar{3}11$ ) crystalline planes of an augite crystal and the (111) crystalline plane of a magnet grain. Therefore, this photo can be viewed as a valid evidence of the growth of augite crystal directly from the surface of the magnet nucleus.

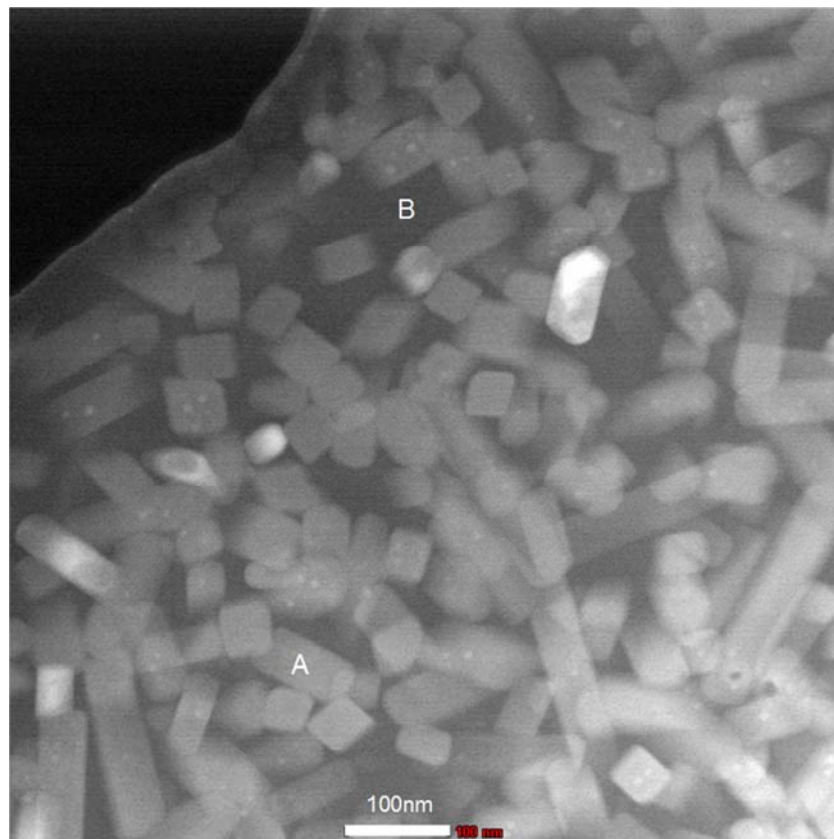
Figure 7 presents the STEM photo of the final obtained glass ceramic sample of the GS0 group and the corresponding EDS spectra of one of the typical light-gray regions and that of the residual glass matrix (dark-grey). It shows the brighter region contains a considerable amount of Ca, Fe, Mg, and Al in addition to higher concentrations of Si and O. This combination is consistent with the compositional assemblage of an augite crystal, indicating the examined light grey region is one augite crystal. Moreover, this photo also shows augite crystals in form of short column intertwines with each other, and the rectangular shape of their cross section is also in accordance with the fact the crystalline structure belongs to the monoclinic system. Contrarily, the dark grey residual glass matrix mainly composes of Si and O in addition to just

fractions of Ca, Fe, Mg. This unusual residual glass matrix of high Si concentration together with the intertwined augite microcrystals should be the main factor contributing to the

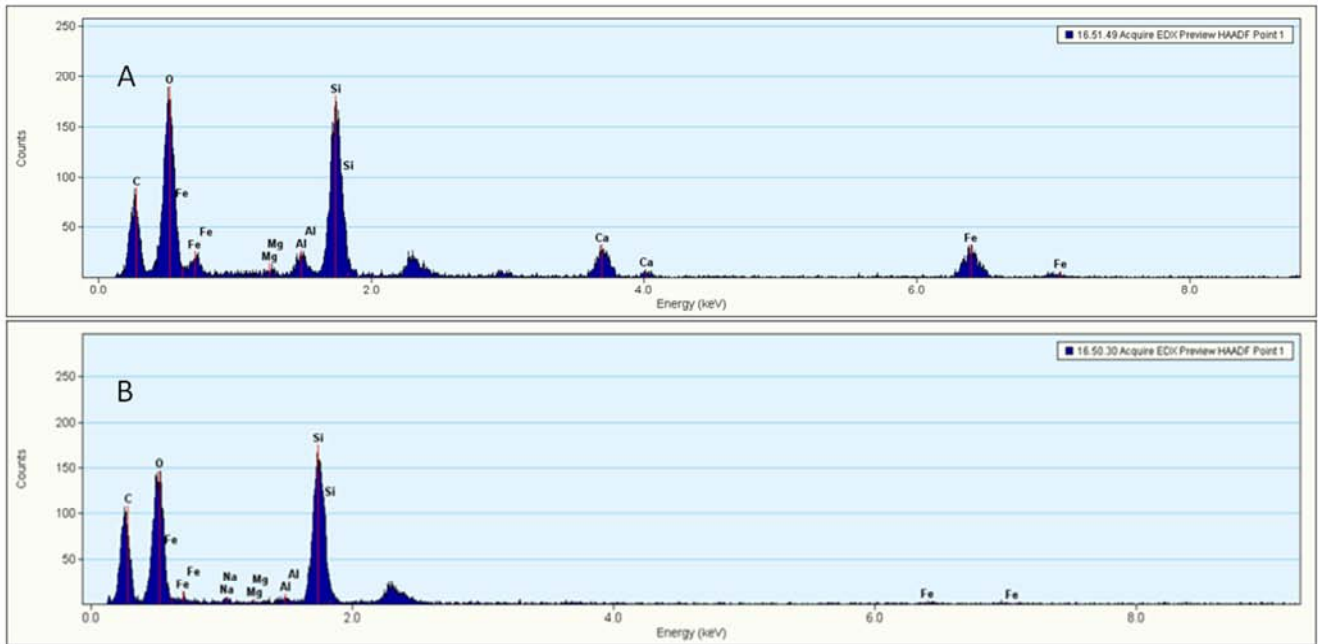
high hardness and bending strength, outstanding resistance to abrasion, and strong stability against acid or alkaline erosion of the special glass ceramic addressed in this study.



*Figure 6. HRTEM photo of the crystallized GS0 sample.*



(a) STEM photo



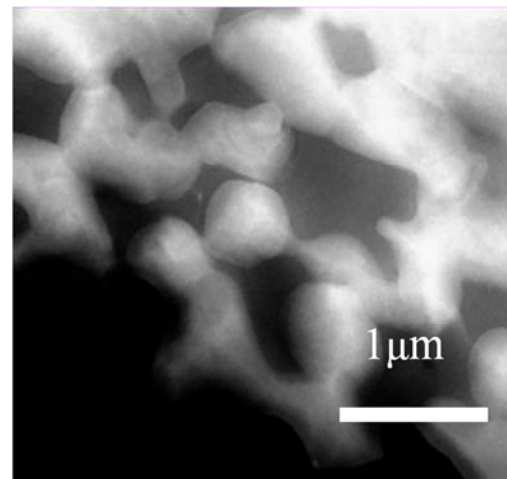
b) EDS result of point A and B as present by photo (a)

Figure 7. STEM photo of crystallized GS0 sample and the EDS results of the investigated points marked out by A and B on the STEM photo.

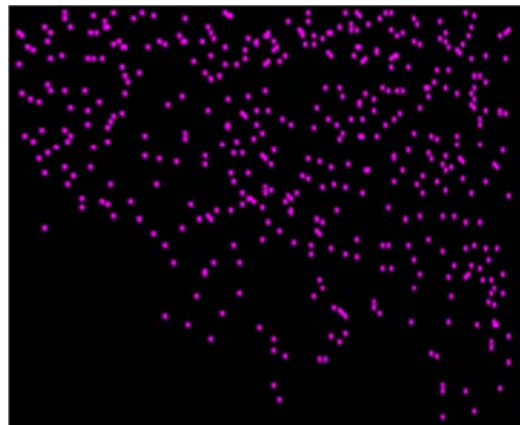
### 3.3. Effect of La/Ce Composite

As one of the well-known modifiers in glass, Rare Earth (RE) ions can promote the clustering of other cations because of their high-field strength. As a result, RE ions can affect both the connectivity of a glass and its latter crystallization process. However, how a RE ion takes its effect relates to how it may exist in a glass. Considerable peer studies have shown a RE ion may exist in the structure of a glass as a substituting ion, interstitial ion or within a newly formed crystalline phase after the addition of RE ion [26-30]. To further verify the in-situ mechanism of La and Ce, the most common RE ion within Bayan Obo mine and its tailing, one sample of GS1 group was crystallized and examined using a STEM (high-angle annular dark field-HAADF mode) and its EDS attachment. The result was present in Figure 8.

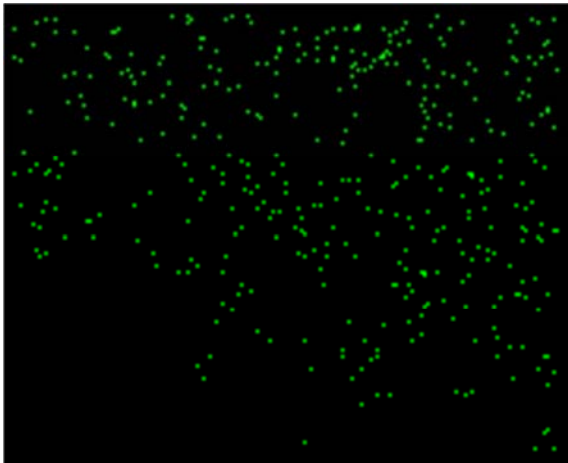
The HAADF photo present in Figure 8 shows there are a great deal of augite grains (bright in contrast) embedding within the matrix of residual glass (dark in contrast). It is worth noticing the shape of augite grains has transformed into the one resembling island with round corners. The corresponding EDS results present in Figure 8 b) and c) exhibit the concentration of La and Ce within the augite crystal are generally higher than that of the neighboring residual glass matrix. Because the size of  $\text{Ca}^{2+}$  ion ( $1\text{\AA}$ ) within the augite crystalline structure with six coordination is similar to that of  $\text{La}^{3+}$  and  $\text{Ce}^{3+}$  ions ( $1.03$  and  $1.01\text{\AA}$  respectively), thus these EDS results can indicate that considerable portion of  $\text{Ca}^{2+}$  ions within the augite crystal have been substituted by those of  $\text{La}^{3+}$  and  $\text{Ce}^{3+}$ .



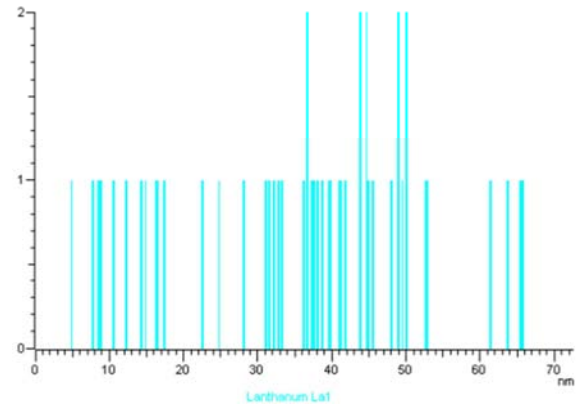
(a) HAADF



(b) La

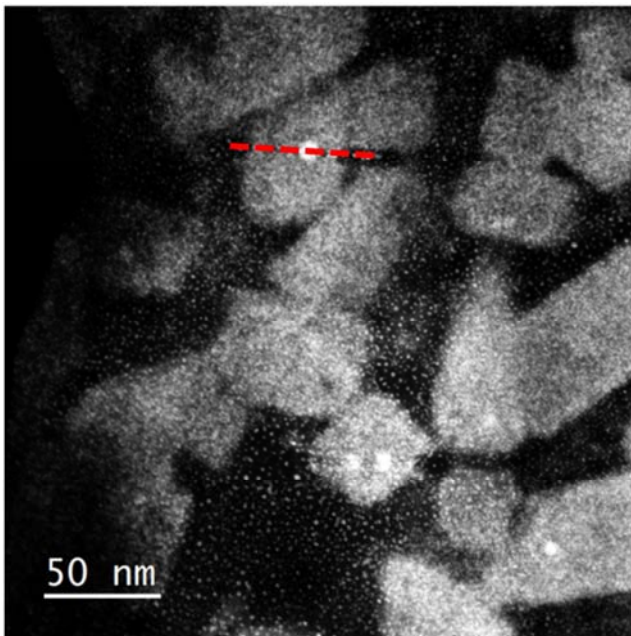


(c) Ce

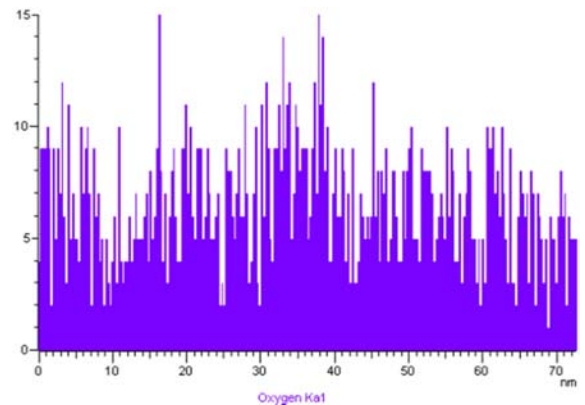


(c) La

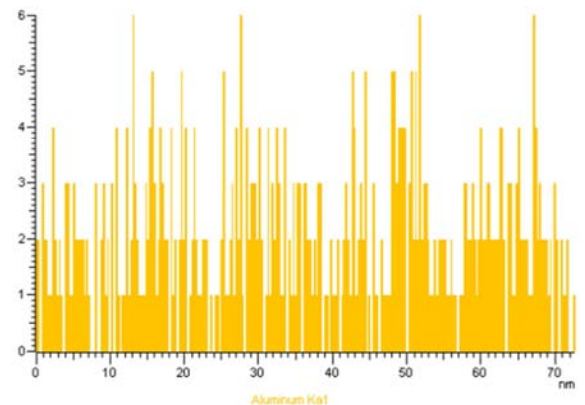
Figure 8. (a) HAADF-STEM photo of the crystallized GSI sample and the corresponding EDS mapping results of (b) La and (c) Ce.



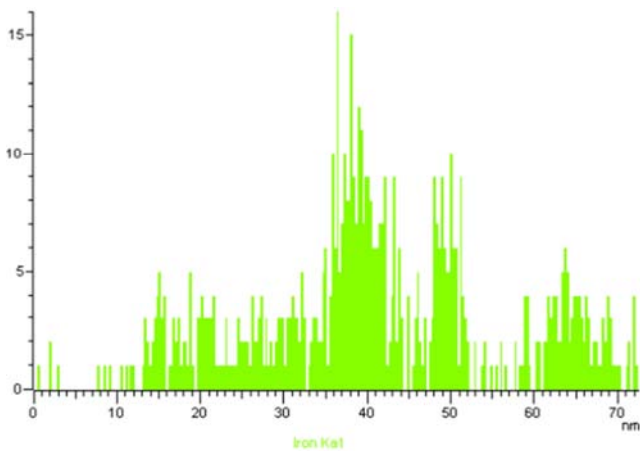
(a) HAADF



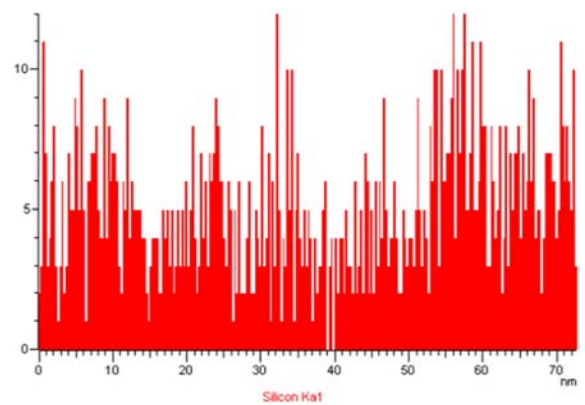
(d) O



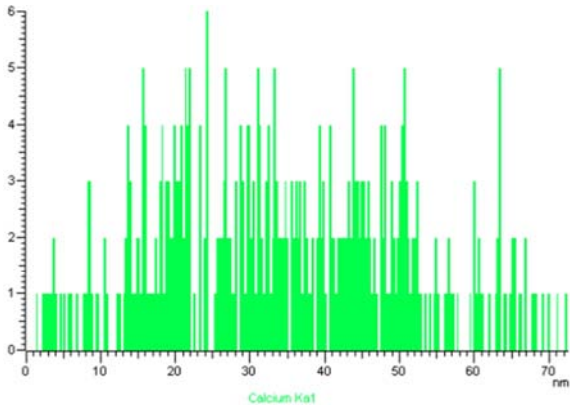
(e) Al



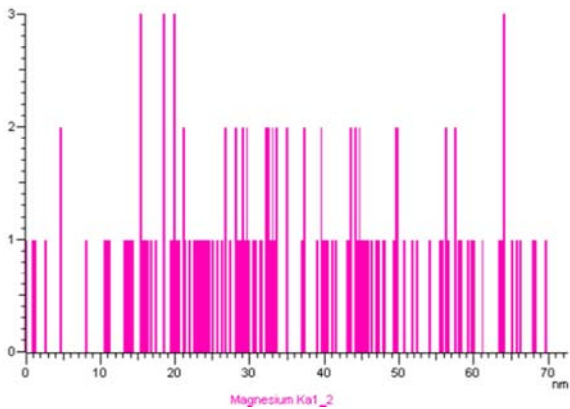
(b) Fe



(f) Si

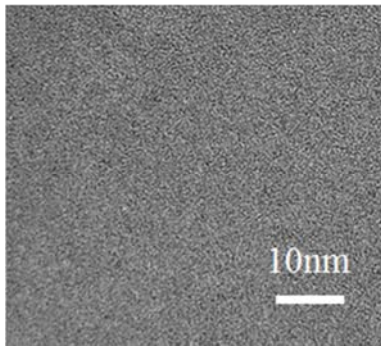


(g) Ca

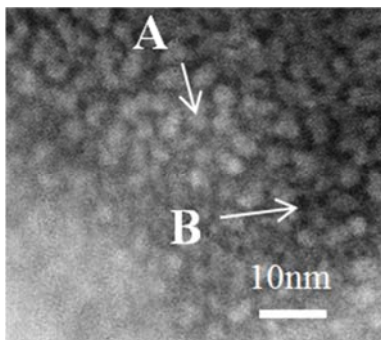


(h) Mg

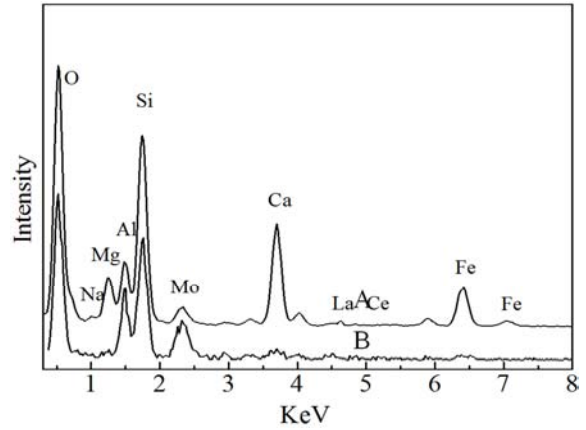
**Figure 9.** STEM-HAADF photo of crystallized GS1 sample (a) and the EDS line scan result along the line on this photo, showing the distribution of (b) Fe, (c) La, (d) O, (e) Al, (f) Si, (g) Ca and Mg on the line.



(a) GS0



(b) GS1



(c) EDS results of tested point A and B

**Figure 10.** STEM-HAADF photo of the typical residual glass region within the crystallized GS0 (a) and GS1 samples (b) and the corresponding EDS result marked by A and B on the photo (b).

In order to reveal the effect of La/Ce ions on nucleation, one sample of GS1 group was heated to the crystallization temperature at a heating rate of 5°C/min and then quenched in water. The resultant sample was examined by the aforementioned STEM in the HAADF mode. The corresponding results were shown in Figure 9. The picture (a) in this figure exhibits some Fe-bearing augite micro-crystals have white spherical particles within the center area. The corresponding EDS line scan results (Figure 9 b~f) show the concentrations of Fe and La within the examined the as tested white particle are higher than those of its neighboring area. Contrarily, no localized enrichment appears in the EDS line scanning results for O, Ca, Al, Mg and Si. As it has been present in the earlier part of this paper, magnet particles can serve as the heterogeneous nucleating center for the crystallization of augite grains within the glass of the Fe bearing pyroxene system. That result and the results in this section in combination indicate portions of La<sup>3+</sup> ion may dissolve into above magnet nuclei through substituting Fe<sup>3+</sup> ions by those of ions of La. Therefore, La ions may exhibit a certain degree of synergetic effect with Fe ions on enhancing the latter crystallization of augite grains.

The STEM-HAADF photo of one of the typical residual glass regions of the above-mentioned GS1 sample was present in Figure 10 in addition to that of GS0 sample obtained through the same process. Figure 10 (a) shows the residual glass region in GS0 sample has a uniform contrast (in grey color). Meanwhile, the residual glass region in GS1 sample has a considerable amount of white spherical regions, indicating they contain more atoms of higher Z number. The corresponding EDS result shown as Figure 10 (c) exhibits the concentrations of ions of Ca and Fe in those white spherical regions are higher than those of the neighboring areas and the ion assemblages of these brighter regions are similar to that of augite crystal. A more magnified HRTEM photo of one of those white spherical regions was shown in Figure 11.

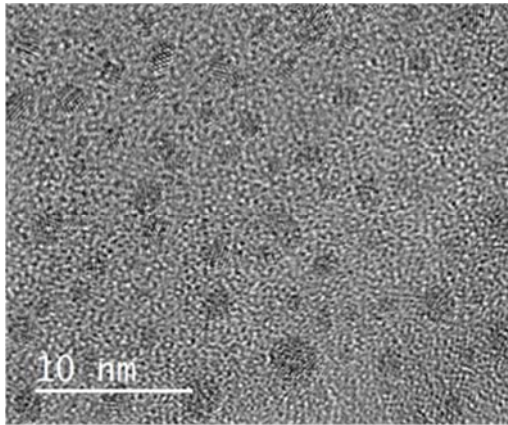


**Figure 11.** HRTEM photo of a typical residual glass region within the crystallized GS1 sample.

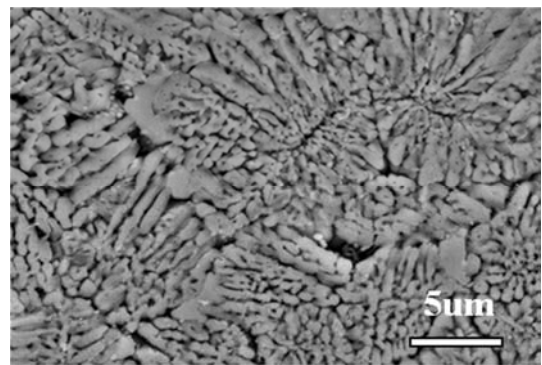
It shows those white regions of an averaged diameter of 2~3nm all contain orderly aligned atoms. As a result, they can be considered as nano-augite crystals. As a lot of  $\text{Ca}^{2+}$ ,  $\text{Fe}^{3+}$  and  $\text{Na}^+$  ions which may decrease the connectivity of glass network, concentrate within those nano-augite crystals, the concentration of Si in the neighboring residual glass will be considerably higher than its normal level. This result can become an important factor contributing to the enhancement in the strength, hardness of the residual glass and its resistances to acid or alkaline erosion.

### 3.4. Effect of Niobium

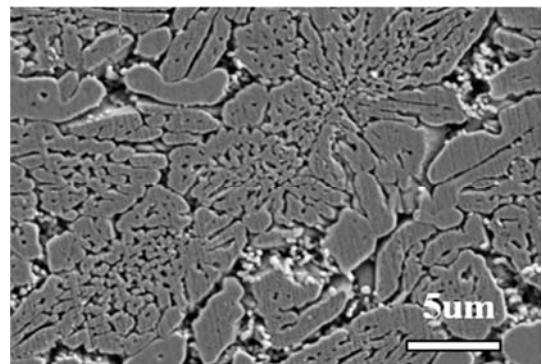
Niobium is one of the typical valuable elements still remaining within Bayan Obo tailing.  $\text{Nb}^{5+}$  cation has strong field strength. Therefore, it should act like aforementioned ions of RE elements on influencing both the microstructure and the properties of the final product theoretically. To examine its effect, samples of GS0' (without intentionally added  $\text{Nb}_2\text{O}_5$ ) and GS2 (with intentionally added 0.5wt%  $\text{Nb}_2\text{O}_5$ ) groups were crystallized under the same condition and examined by the SEM mentioned in section 2, and the result was present in Figure 12.

As shown in Figure 12 a), the shape of diopside dendrite, the primary crystalline phase identified in the final heat-treated GS0' sample, closely resembles that of a chrysanthemum flower. Dendrite crystal of such shape is normally the result of a glass having low viscosity and being lack of nuclei during the slow cooling process of the glass melt [31]. With the addition of  $\text{Nb}_2\text{O}_5$  in GS2 sample, the average size of those diopside dendrites decrease. Peer study has shown Nb cations can act as nucleation enhancer, which may enhance the crystallization of the primary phase within a glass of the similar composition [32]. Therefore, the result in this section suggests similar mechanism may be taking effect as well in this study, causing the average size of primary crystalline grains to decrease. Another morphological change with the addition of  $\text{Nb}_2\text{O}_5$  is the formation of some diopside grains resembling an island with round corners. This phenomenon indicates the viscosity of the glass melt increase with the addition of  $\text{Nb}_2\text{O}_5$ , thereby inhibiting the fast

diffusion of ions required by fast growth of dendrite crystals. The reason behind this morphology change should relate to the fact that niobium ions normally exist with the aluminosilicate based glass in form of  $[\text{NbO}_6]$  octahedral. Because such structure unit has one negative effective charge, it can automatically attract cations, such as  $\text{Ca}^{2+}$  or  $\text{Fe}^{3+}$ , to its vicinity to keep the electrol neutrality. As a result, the composition around niobium ions may become more favorable for the formation of diopside crystals. This should be a factor to be considered as well for the comprehensive appreciation of the effect of niobium. This phenomenon should also be the synergetic mechanism of niobium ions with those of calcium and iron on influencing the microstructure and properties of the slag glass ceramics investigated in this paper.

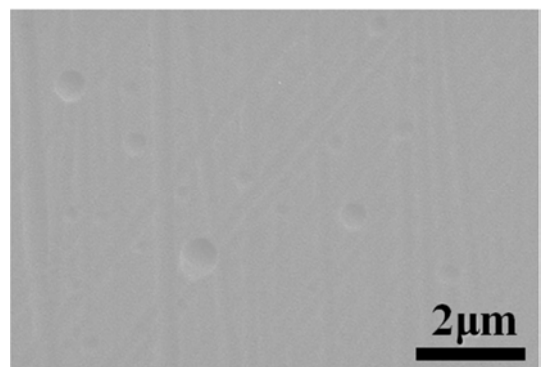


(a) GS0'

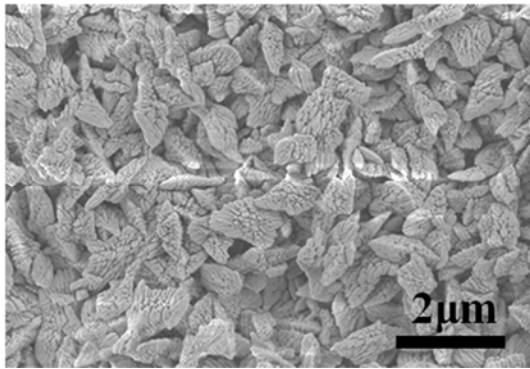


(b) GS2

**Figure 12.** SEM photos of the crystallized GS0' and GS2 sample.



(a) Conventionally Crystallized



(b) Crystallized by microwave heating

**Figure 13.** SEM pictures of GS0' sample crystallized at 670°C for two hours in a traditional electric resistance furnace (a) and the sample with the same composition crystallized at the same temperature by microwave heating for 20 minutes.

### 3.5. Effect of Microwave Heating

The practice of adapting the above mentioned laboratory procedure for glass ceramic articles fabrication at a larger scale, such as in a pilot plant or in an industrial manufacturing line, has shown the energy consumed by the heat-treatment procedure must be reduced in order to lower the cost of manufacturing. Microwave heating is well known for its fast heating rate [33]. Therefore, it is possible to apply this technique in the crystallization process to save manufacturing time. To test this theory, two GS0' samples were crystallized, in which one is crystallized at 670 °C for two hours using the conventional electrical resistance heating, another one using microwave heating at the same temperature but for only 20 minutes. The SEM photos of these two resultant samples were present in Figure 13. It is obvious the conventionally crystallized sample (Figure 13 a) contains no observable crystals on its cross section surface after the as defined crystallization process. Contrarily, in the sample crystallized by microwave heating, there are already a considerable amount of crystals with similar morphological feature as the one shown in Figure 12 a, although their average size is much smaller. This result means microwave heating can reduce both the temperature and time for crystallization treatment in the manufacturing process of glass ceramics when compared with the conventional electric resistance heating method.

## 4. Conclusion

Near two decades of the research work of the research group of the current authors has shown it is possible to fabricate a special slag glass ceramics with high hardness and bending strength, good resistance to abrasion and strong stability against acid or alkaline erosion from Bayan Obo tailing and a fly ash collected in one of the local thermal power plants. The compositional complexity of this waste derived material entitles it to be considered as a high-entropy material. Meanwhile, the results of the research group of the current authors has shown that industrial solid wastes, such as Bayan Obo tailing and fly ash, can be used as raw materials to

fabricate glass ceramics with general superior properties. This is a feasible way to reuse industrial wastes as resources. During the process of fabricating glass ceramic of the augite system from Bayan Obo tailing and fly ash, Fe ions can promote the nucleation of augite through the formation of magnet particles as heterogeneous nuclei, in which Fe ions can be partially substituted by those of La. This is one form of synergetic effect of Fe and La on influencing both microstructure and properties of the material. With the addition of La/Ce composite oxide, clusters of La, Fe and Ca-rich crystals of two to three nanometers can form within the residual glass region of augite glass ceramics. Meanwhile, the composition of the rest of the residual glass will become richer in SiO<sub>2</sub>. This is one of the mechanisms to improve the physical and chemical properties of the residual glass with augite glass ceramics. Moreover, ions of La and Ce can partially substitute cations of Ca in augite crystal. Doping Nb to the diopside glass ceramics can decrease the average size of diopside crystals and promote the formation of such crystals resembling an island with round corners. Compared with the traditional electric resistance heating, microwave heating can remarkably reduce the temperature and time required for the crystallization of the as investigated glass ceramics in this study.

Above results can theoretically and practically promote the practice of reusing industrial solid wastes as resources for the fabrication of useful material with high added value.

## Acknowledgements

This study is funded by the “Inner Mongolia Science & Technology Plan Projects (0901051701 and 0406091701). This study is also supported by the residue fund of the 973 Program with the grant number 2012CB722802. Sponsorship from the “Inner Mongolia Autonomous Region Science and Technology Major project: Fundamental and key technology research for the integrated exploitation of Bayan Obo Mine with high added value” and “Inner Mongolia autonomous region scientific innovation team of integrated exploitation of Bayan Obo mine multi-metal resource” are also fully acknowledged by all authors of current study. This study is also supported by “The IMUST Innovation Fund (No. 2017QDL-S03).

## References

- [1] Yongdan C., Zhao C., and Jie L., et al. (2013). Current study situation and development on flotation of rare earth in Bayan Obo Mine. *Mining & Processing Equipment* 41, 93-96. (in Chinese).
- [2] Jian Zhong C., Yun Bing H., and Li Ping C., (2007). Making Rational Multipurpose Use of Resources of RE in Baiyun Ebo Deposit. *Rare Earth* 28, 70-74 (in Chinese).
- [3] Du Y. S., Yang X. W., and Zhang H. X., et al (2016). Effect of heat treatment on the crystallization toughening of tailing-derived glass-ceramics. *Journal of Ceramics Process Research* 17, 1234-1248.

- [4] Bao Wei L., Yong Sheng D., and Xue Feng Z., et al (2015). Crystallization characteristics and properties of high-performance glass-ceramics derived from baiyunebo east mine tailing. *Environmental Progress & Sustainable Energy* 34, 420-426.
- [5] Hua C., Bao Wei L., and Ming Z., et al. (2015). Effect of existence form of  $\text{La}^{3+}$  on the properties of the Bayan Obo Mine tailing glass ceramics. *Acta Physica Sinica* 64, 196201-196208 (in Chinese).
- [6] Bao Wei L., Lei Bo D., and Xue Feng Z., et al (2015). Preparation and corrosion behavior of glass-ceramics tubes made of Bayan Obo tailings and fly ash. *International Journal of Applied Ceramic Technology* 12 (S1), 41-48.
- [7] Bao Wei L., Hong Xia L., and Xue Feng Z., et al (2015). Nucleation and crystallization of tailing-based glass-ceramics by microwave heating. *International Journal of Minerals, Metallurgy, and Materials* 22, 1342-1349.
- [8] Bao Wei L. Yong Sheng D., and Yue Feng Z., et al (2013). Effects of iron oxide on the crystallization kinetics of Baiyunebo tailing glass-ceramics. *Transactions of the Indian Ceramic Society* 72, 119-123.
- [9] Bao Wei L., Lei Bo D., and Xue Feng Z., et. al. (2013). Structure and performance of glass-ceramics obtained by Bayan Obo tailing and fly ash. *Journal of Non-Crystalline Solids* 380, 103-108.
- [10] Bernardo E., Dattoli A., and Bonomo E., et al. (2011). Application of an industrial waste glass in "glass-ceramic stoneware". *International Journal of Applied Ceramic Technology* 8, 1153-1162.
- [11] Karamanov A., Pelino M., and Salvo M., et al. (2003). Sintered glass-ceramics from incinerator fly ashes. Part II. The influence of the particle size and heat-treatment on the properties. *Journal of the European Ceramic Society* 23, 1609-1615.
- [12] Cheng T. W., and Chiu J. P. (2003). Fire-resistant geopolymers produced by granulated blast furnace slag. *Minerals engineering* 16, 205-210.
- [13] Cheng T. W., Ueng T. H., and Chen Y. S., et al (2002). Production of glass-ceramic from incinerator fly ash. *Ceramics International* 28, 779-783.
- [14] Park Y J., and Heo J. (2002). Conversion to glass-ceramics from glasses made by MSW incinerator fly ash for recycling. *Ceramics International* 28, 689-694.
- [15] Cimdin R., Rozenstruha I., and Beraina L., et al (2000). Glass ceramics obtained from industrial waste. *Resources, Conservation and Recycling* 29, 285-290.
- [16] Romero M., Rawlings R. D., and Rincon J. M. (1999). Development of a new glass-ceramic by means of controlled vitrification and crystallisation of inorganic wastes from urban incineration. *Journal of the European Ceramic Society* 19, 2049-2058.
- [17] Carter S., Ponton C. B., and Rawlings R. D., et al (1988). Microstructure, chemistry, elastic properties and internal friction of Silceram glass-ceramics. *Journal of Materials Science* 23, 2622-2630.
- [18] Boccaccini A. R., and Kopf M, Stumpfe W. (1995). Glass-ceramics from filter dusts from waste incinerators. *Ceramics International* 21, 231-235.
- [19] Pisciella P., and Pelino M. (2005). FTIR spectroscopy investigation of the crystallisation process in an iron rich glass. *Journal of the European Ceramic Society* 25, 1855-1861.
- [20] Karamanov A., Taglieri G., and Pelino M. (1999). Iron-rich sintered glass - ceramics from industrial wastes. *Journal of the American Ceramic Society* 82, 3012-3016.
- [21] Lonroth N., and Yue Y. Z. (2008). Structural order and crystallization of an iron-rich aluminosilicate liquid under oxidizing condition. *Journal of Non-Crystalline Solids* 354, 1190-1193.
- [22] Karamanov A., and Pelino M. (2001). Crystallization phenomena in iron-rich glasses. *Journal of Non-Crystalline Solids* 281, 139-151.
- [23] Francis A. A. (2006). Crystallization kinetics of magnetic glass-ceramics prepared by the processing of waste materials. *Materials Research Bulletin* 41, 146-1154.
- [24] Sharma K., Singh S., and Prajapat C. L., et al. (2009). Preparation and study of magnetic properties of silico phosphate glass and glass-ceramics having iron and zinc oxide. *Journal of Magnetism and Magnetic Material* 321, 3821-3828.
- [25] Wang S M, Kuang F H, and Yan Q Z, et al. (2011). Crystallization and infrared radiation properties of iron ion doped cordierite glass-ceramics. *Journal of Alloys and Compounds* 509, 2819-2823.
- [26] Garai M., Karmakar B. (2016). Rare earth ion controlled crystallization of mica glass-ceramics. *Journal of Alloys and Compounds*, 678, 360-369.
- [27] Goel A, Tulyaganov D. U., and Kharton V. V., et al. (2008). The effect of  $\text{Cr}_2\text{O}_3$  addition on crystallization and properties of  $\text{La}_2\text{O}_3$ -containing diopside glass-ceramics, *Acta Materialia* 56, 3065-3076.
- [28] Lu P, Zheng Y., and Cheng J. S., et al. (2013). Effect of  $\text{La}_2\text{O}_3$  addition on crystallization and properties of  $\text{Li}_2\text{O}-\text{Al}_2\text{O}_3-\text{SiO}_2$  glass-ceramics, *Ceramics International* 39, 8207-8212.
- [29] Chen L., Yu C. L., and Hu L. L., et al. (2013). Effect of  $\text{La}_2\text{O}_3$  on the physical and crystallization properties of  $\text{Co}^{2+}$  doped  $\text{MgO}-\text{Al}_2\text{O}_3-\text{SiO}_2$  glass. *Journal of Non-Crystalline Solids* 360, 4-8.
- [30] Luo Z. W., Lu A. X., and Han L. G. (2009). Effects of doping  $\text{La}_2\text{O}_3$  on crystallization and mechanical properties of lithium disilicate glass-ceramics. *The Chinese Journal of Nonferrous Metals* 19, 2018-2023.
- [31] Pinckney L. R., and Beall G. H. (2008). Microstructural evolution in some silicate glass-ceramics: A Review. *Journal of the American Ceramic Society* 91, 773-779.
- [32] Denry I. L., Holloway J. A., and Nakkula R. J., et al (2005). Effect of niobium content on the microstructure and thermal properties of fluorapatite glass-ceramics. *Journal of Biomedical Materials Research Part B* 75, 18-24.
- [33] H. J. Kitchen, S. R. Vallance, and J. L. Kennedy, et al. Carassiti, A. Harrison, A. G. Whittaker, T. D. Drysdale, S. W. Kingman, D. H. Gregory (2014). *Modern Microwave Methods in Solid-State Inorganic Materials Chemistry: From Fundamentals to Manufacturing*. *Chemical Reviews* 114, 1170-1206.